

SciEn Conference Series: Engineering Vol. 3, 2025, pp 420-424

https://doi.org/10.38032/scse.2025.3.114

Enhancing Low-Velocity Wind Energy Harvesting through Semi-Circular Passive Turbulence Controls on Bluff Bodies

Md. Mohiuddin^{1,*}, Zahir U. Ahmed¹, Mohammad Ilias Inam¹, Md. Rhyhanul Islam²

¹ Department of Mechanical Engineering, Khulna University of Engineering & Technology, Khulna-9203, Bangladesh

ABSTRACT

The exponential growth of small-scale electronic devices and the limitations of battery life that necessitate frequent replacements in remote locations have driven researchers to develop various energy harvesting techniques. Conventional wind turbines are inefficient for capturing low-velocity wind energy due to their complexity and dependence on high wind speeds. Therefore, vortex-induced energy harvesting has attracted considerable attention as an alternative, but its performance is highly dependent on wind velocity, generating high output power in a narrow range and almost none at other velocities. This study aims to enhance this range by integrating two semi-circular passive turbulence control (SPTC) devices at different circumferential positions on a cylindrical bluff body, symmetrically aligned with the stagnation line. Experimental studies conducted in a subsonic wind tunnel demonstrated that while SPTC placements at 45° and 90° reduced performance, positions at 60° and 75° significantly expanded the operational range and increased output power. These configurations also showed continuous power increases with wind speed, offering a potential solution to the limitations of traditional cylindrical bluff bodies.

Keywords: Energy Harvesting; Vortex-Induced Vibration; Flow-Induced Vibration; Piezoelectricity; Low Velocity; Cantilever; Passive Turbulence Control (PTC).



Copyright @ All authors

This work is licensed under a Creative Commons Attribution 4.0 International License.

1. Introduction

The rising demand for energy contributes to increased pollution due to the extensive use of fossil fuels. This environmental impact compels researchers to focus on renewable energy solutions. Due to the bulkiness and limited lifespan of batteries, there is a growing interest in small energy harvesters that can be integrated with IoT devices. Energy harvesting is the process of capturing ambient energy sources such as vibrations, temperature variations, solar radiation, and wind to convert them into electrical power. Among these techniques, harnessing wind energy has always been popular due to its unlimited availability. However, conventional wind turbines require high wind velocities and involve complex structures, which makes them unsuitable for harnessing low wind velocities in IoT applications [1]. Consequently, researchers are exploring alternative methods for wind energy harvesting, which results in the development of flow-induced vibration (FIV) technologies. FIV encompasses various mechanisms, including vortex-induced vibration (VIV).

VIV occurs when fluid flows, typically around a cylindrical object, causing vortices to form alternately on each side of the object. This alternating vortex shedding exerts a cyclic aerodynamic force, which causes the structure to vibrate. However, the aerodynamic force due to vortex shedding is very small, leading to a vibration with a very smaller amplitude. The frequency of vortex shedding is represented by $f = (US_t/D)$, where f depends on the flow velocity U and Strouhal number S_t and matches the energy harvester's resonant frequency at a particular flow speed [2]. When the cyclic aerodynamic force becomes equal to or comes close to the harvester's natural frequency, it significantly amplifies the

vibration, which can be converted to electricity using electromagnetic, piezoelectric, electrostatic, dielectric, or triboelectric conversion methods [3]. Since the shedding frequency is proportional to flow velocity, the matching between the natural frequency and shedding frequency usually occurs at a lower wind speed, which makes VIV harvesters ideal for capturing energy from slow-moving flows [4]. This requirement for frequency alignment has divided research into two main areas: maximizing harvested energy and expanding the operational velocity range.

Dai et al. [5] introduced a nonlinear model using a partially coated cantilever beam with piezoelectric material and attached to a cylindrical bluff body at its free end. Cantilever beams are widely used in strain-driven energy harvesters due to their high energy conversion efficiency, ease of controlling the natural frequency, and the potential for improving output simply by optimizing the cantilever shape et al. [9] [6]–[8]. Azadeh-Ranjbar demonstrated experimentally that increasing the length-to-diameter ratio of the cylinder improves the bandwidth of the lock-in region and deflection magnitude. Gao et al. [10] found that surface roughness on the bluff body leads to increased displacement and harvested energy. In contrast, Huang et al. [11] reported a 64% reduction in VIV when helical grooves were applied to the bluff body. Jin et al. [12] enhanced the performance of the VIV harvester by adding biomimetic shapes to the cylindrical bluff body, which increased both power output and the lockin region. Similarly, Wang et al. [13] showed that applying a convex metasurface can increase maximum voltage output by 15.56% and expand the operating range by 63.64%. Additional experiments by the same team revealed that adding

² Department of Mechanical Engineering, Iowa State University of Science and Technology, Ames, IA 50011, USA

concave metasurfaces resulted in a 9.44% increase in voltage output and a 30.77% increase in bandwidth [4]. In another study, Song et al. [14] found that attaching a split plate behind the bluff body improved the bandwidth of the operating range but reduced the output voltage.

Further research by Wang et al. [15] investigated the use of passive turbulent control (PTC) devices on VIV harvesters, concluding that the proper placement and size of these PTCs could significantly improve the working range and voltage output. In this context, PTCs refer to rough surface modifications on the bluff body. Hu et al. [16] experimented with a configuration involving two cylindrical rods positioned symmetrically at a 60-degree angle from the bluff body's stagnation line, which greatly expanded the aeroelastic instability range, enabling energy capture beyond the usual VIV range. Zheng et al. [17] explored the effects of fairing devices on circular cylinders and observed that interactions between VIV and galloping forces allowed galloping to occur at lower speeds. Collectively, these studies show that the shape and design of bluff bodies have both positive and negative impacts on VIV energy harvesters, suggesting that further optimization of bluff body design could enhance energy output in VIV harvesters.

This paper explores performance improvements in flow-induced energy harvesting by integrating two semi-circular passive turbulence controllers (SPTCs) symmetrically along the stagnation line of a cylindrical bluff body, tested under wind tunnel conditions. Although Mohiuddin et al. [18] previously examined passive turbulence controllers with a semi-circular arrangement, their study used a vertical configuration. Prior research has shown that results from vertical arrangements can differ significantly from horizontal ones, suggesting that further investigation using this alternative setup is warranted. In this study, two semi-circular turbulence controllers were attached symmetrically along the stagnation line, with their placement optimized in terms of circumferential angle.

2. Experimental Setup and Procedure of Analysis

The experiment was conducted in a subsonic wind tunnel with dimensions of $305 \times 305 \times 600$ mm³. A hot wire anemometer, with a resolution of 0.1 m/s, was used to capture fine variations in wind velocity. An aluminum frame was constructed to secure the cantilever beam within the wind tunnel, with one end of the beam fastened to the frame and the other end designed to hold the bluff bodies. The cantilever beam, which was also made of aluminum, had dimensions of $125 \times 27.75 \times 0.84$ mm (length × width × thickness), and was kept consistent throughout the experiment to eliminate variations in material properties and dimensions. The bluff bodies were mounted and replaced by unscrewing and reassembling nut-bolt connections.

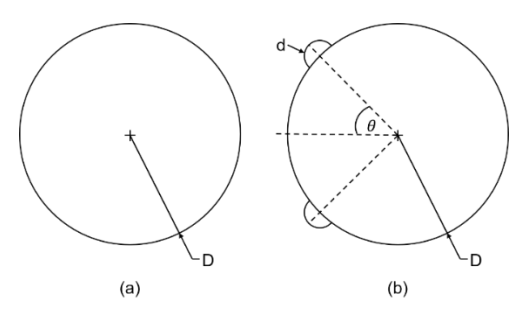


Fig.1 Experimental circular cylinder cross-section. (a) baseline model, (b) with semi-circular PTC.

The bluff bodies were 3D printed using ABS material, each featuring two semi-circular passive turbulence control (SPTC) devices symmetrically positioned relative to the stagnation line, at different circumferential angles (θ), as shown in Figure 1(b). For the experimental study, four bluff bodies were fabricated with θ values of 45°, 60°, 75°, and 90°. A cylindrical bluff body without SPTCs, as shown in Figure 1(a), was also printed to serve as a baseline model, allowing comparison between the energy harvesters with SPTCs and conventional designs. Since variations in the mass of bluff bodies could affect the natural frequency of the energy harvester and lead to unfair comparisons, auxiliary masses were added to ensure all bluff bodies had the same mass.

To measure the continuously changing deflection of the bluff body caused by flow-induced vibrations, a laser displacement sensor (Panasonic HG C-1400) was employed. The sensor was integrated with a data logger (GraphTec GL 240), which recorded the data at a rate of 50 samples per second.

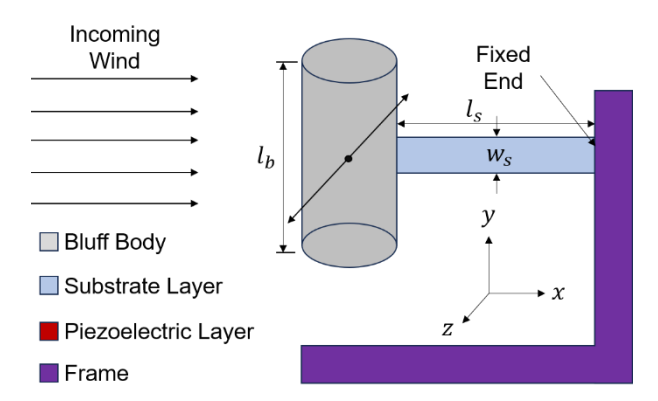


Fig.2 Schematic of circular cylinder-based FIV energy harvester.

To determine the output power of the energy harvester, the following equation was used,

$$P_{out} = 2\pi^2 m f^2 A^2 \tag{1}$$

Where m represents the effective mass of the vibrating system, f is the frequency of vibration, and A is the amplitude of vibration. The amplitude A was determined as the maximum deflection from the data recorded by the data logger. The vibration frequency f was calculated by applying a fast Fourier transform (FFT) to the recorded deflection data of the vibrating system. It is important to note that the output power in this study refers to mechanical energy, which can be converted into electrical energy using piezoelectric materials or other electromechanical conversion methods. However, some energy loss will occur during the conversion process.

3. Results and Discussions

3.1 Baseline Cylindrical Model

Initially, the energy harvester was tested using a conventional cylindrical bluff body without any SPTCs to establish a baseline for comparison with bluff bodies equipped with SPTCs. A free decay test was performed to determine the resonant frequency of the energy harvester. In this test, the bluff body was displaced and then released, allowing it to vibrate freely as the deflection naturally decreased over time. The deflection of the bluff body was recorded throughout this process, as shown in Figure 3(a). The recorded data was then analyzed using Fast Fourier

Transform (FFT), and the results, presented in Figure 3(b), revealed the system's natural frequency to be 4.28 Hz.

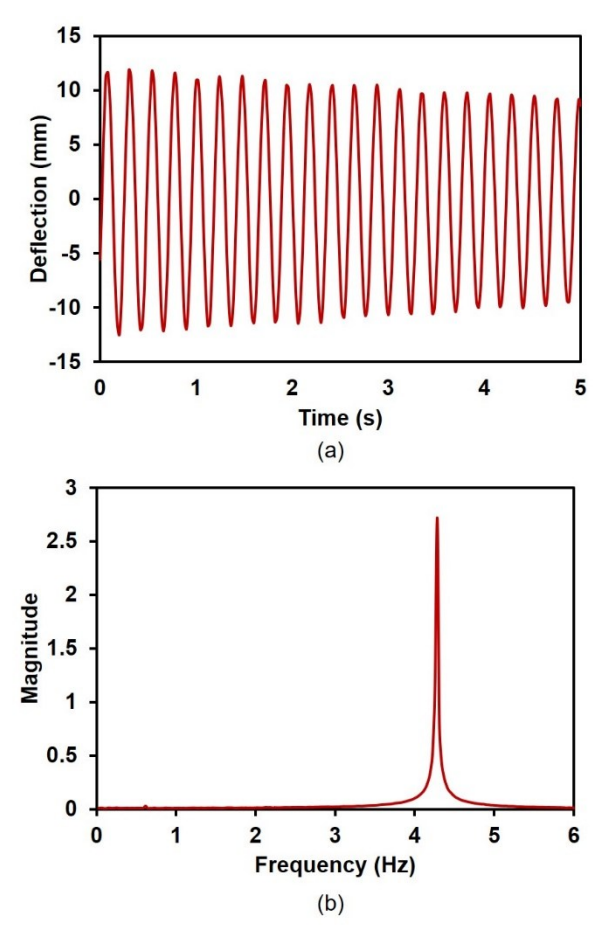


Fig.3 (a) Time history depicting vibrating displacement during the free decay vibration test of the baseline model, (b) FFT analysis of the free decay test.

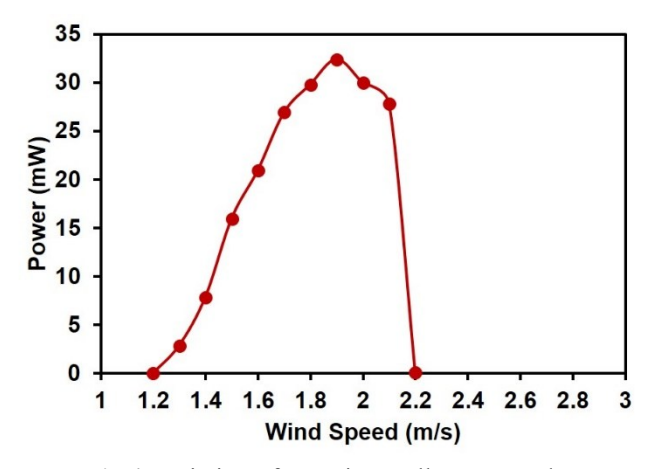


Fig.4 Variation of experimentally measured RMS output voltage with wind speed for the baseline model.

Figure 4 shows that the output power begins to increase at a flow velocity of 1.2 m/s, peaking at 32.41 mW at 1.9 m/s, and then drops sharply, reaching nearly zero at 2.2 m/s. This sudden rise in output power occurs when the vortex shedding frequency matches the natural frequency of the energy harvester. The deflection data of the bluff body at 1.9 m/s, as shown in Figure 5(a), corresponds to the point of maximum output power. The FFT analysis of this data, presented in Figure 5(b), confirms that the energy harvester was vibrating exactly at its natural frequency when producing maximum

power, proving that the vortex shedding frequency at this point was synchronized with the natural frequency of the harvester. Interestingly, once this synchronization—known as frequency locking—occurs, the vortex shedding frequency remains locked to the natural frequency over a small range of flow velocities, causing the output power to stay high between 1.2 m/s and 2.2 m/s. However, when the flow velocity deviates further, the mismatch between the vortex shedding frequency and the natural frequency causes a significant reduction in deflection, leading to a sharp decline in output power.

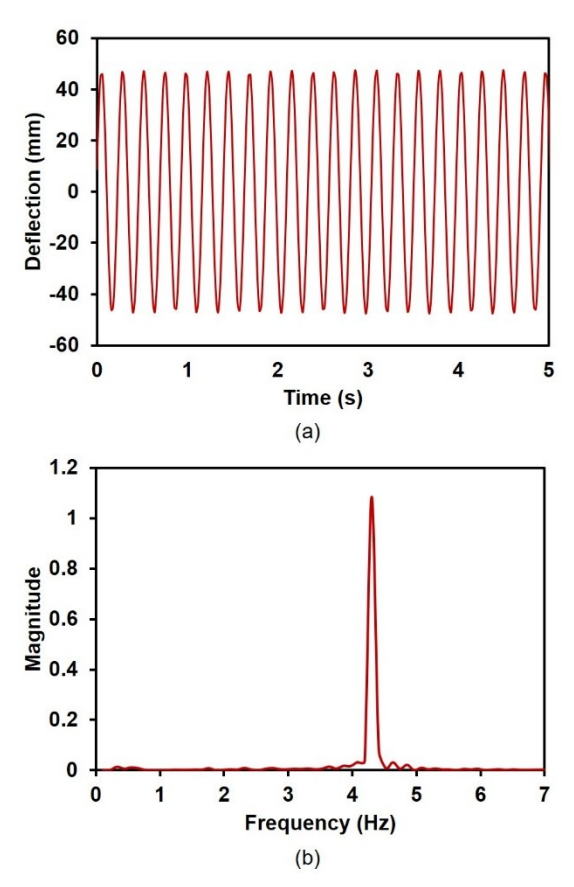


Fig.5 (a) Time history depicting vibrating displacement of the baseline model during 2 m/s wind speed, (b) FFT analysis.

3.2 Semi-circular PTC

Figure 6(a-d) illustrates the variations in output power with wind speed for different circumferential positions of the SPTCs. It is evident that the effective range of flow velocities, within which the output power is higher, can either increase or decrease depending on the circumferential positioning of the SPTCs. This variation in output power is explained by the influence of the SPTCs on the Strouhal number, which directly impacts the vortex shedding frequency. The relationship between the Strouhal number and vortex shedding frequency is given by,

$$f = US_t/D (2)$$

In Figure 6(a), for SPTCs positioned at $\theta=45^\circ$, the maximum recorded output power was 1.3 mW at a wind speed of 0.9 m/s, with an effective velocity range of 0.6 m/s to 1.3 m/s. Compared to the baseline, both the output power and effective bandwidth decreased by 96% and 30%, respectively.

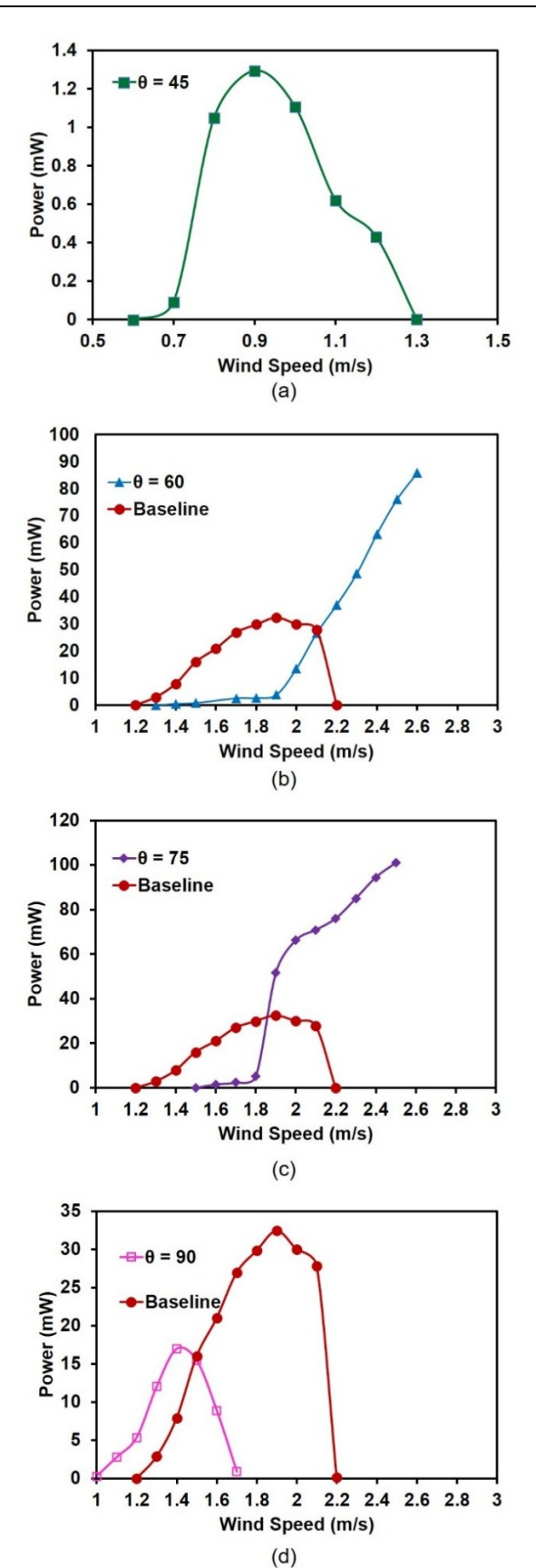


Fig.6 Comparison between the experimentally measured RMS voltage of the baseline model and semi-circular PTC at (a) 30°, (b) 45°, (c) 60°, (d) 75°.

Similarly, at $\theta = 90^{\circ}$, the maximum output power was 16.98 mW, about 48% lower than the baseline, with a 30% reduction in effective bandwidth. These results clearly show that placing SPTCs at $\theta = 45^{\circ}$ and 90° offers no improvement

in terms of either output power or bandwidth, except the fact that providing substantial output compared to other configurations at a lower velocity.

This behavior is due to the influence of the SPTCs on the shape of the shear layer, which affects the lock-in region of vortex-induced vibrations (VIV), as reported by Wang et al. [15]. The addition of PTC directly affects the separation point, thereby change the vortex-shedding pattern. In these cases, the modified shear layer increases the Strouhal number, and as the equation suggests, a higher Strouhal number causes the vortex shedding frequency to change more rapidly with the flow velocity. This explains why the peak power is achieved earlier at $\theta = 45^{\circ}$ and 90° compared to the baseline model. However, since the shedding frequency changes rapidly with velocity, it quickly moves away from the natural frequency of the energy harvester, leading to a smaller effective bandwidth. Additionally, because the frequency matching occurs at lower velocities, the aerodynamic force driving the harvester's vibrations within the effective bandwidth is weaker, as it is proportional to the square of the flow velocity. This results in reduced output power in these configurations.

The analysis of output power from the energy harvester with SPTCs positioned at $\theta = 60^{\circ}$ and 75° revealed a distinctly different behavior compared to the conventional vortex-induced energy harvester, as shown in Figure 6(b, c). Instead of the output power peaking and then decreasing with increasing wind speed, as in typical VIV harvesters, the power continued to rise after a certain minimum velocity. This phenomenon cannot be solely attributed to vortex shedding. Rather, it may be due to the onset of galloping, as explained by Hu et al. [19], who studied the effect of circular and triangular PTCs in this context. Two possible explanations arise from this observation. The first is that VIV occurred during the early part of the lock-in region, and galloping began before the output voltage could decrease, leading to a continued increase in voltage with wind speed. The second possibility is that VIV did not occur at all at $\theta =$ 60° and 75°, and galloping was triggered at a much lower velocity than usual. This behavior differs from conventional galloping, which typically dominates at higher wind speeds. In either case, it can be concluded that positioning the semicircular PTCs at $\theta = 60^{\circ}$ and 75° induces galloping much earlier than in traditional setups. This early transition significantly enhances both output power and the previously limited effective bandwidth. However, it should be noted that these configurations result in substantial output power being achieved at relatively higher velocities, which could pose a challenge, as flow-induced energy harvesters are generally designed to operate in low-velocity wind conditions.

4. Conclusion

This experimental study examined the impact of adding two SPTC devices at various circumferential positions on a cylindrical bluff body aligned with the stagnation line of a horizontally aligned FIV cantilever energy harvester. By analyzing SPTC placements at 45°, 60°, 75°, and 90°, it was found that the circumferential position of the SPTCs critically influences both the output power and the operational range of wind speeds. Specifically, SPTCs positioned at 45° and 90° showed a suppressive effect on the harvester's performance, leading to a reduction in both peak output power and effective bandwidth. In contrast, SPTC configurations at 60° and 75° notably enhanced the

harvester's performance, expanding the bandwidth and continuously increasing output power with rising wind speeds. The performance variations observed at different SPTC positions can be attributed to alterations in the shear layer dynamics, which influence the Strouhal number and consequently the vortex shedding frequency. For SPTCs at 45° and 90°, the increased Strouhal number leads to a rapid mismatch between the shedding frequency and the natural frequency of the energy harvester, which results in reduced performance. However, at 60° and 75°, the SPTCs cause a change in flow dynamics, which leads to the onset of galloping within the lock-in region. The result of this phenomenon is a continuous increase in output power with wind speed rather than the typical peak-and-decline pattern of conventional VIV harvesters. The unique behavior at 60° and 75° demonstrates that specific SPTC placements not only improve effective velocity range but also notably enhance power generation. However, further investigations are required for obtaining the optimal size of SPTCs relative to bluff body dimensions, as this could lead to even greater performance improvements.

References

- [1] A. Tummala, R. K. Velamati, D. K. Sinha, V. Indraja, and V. H. Krishna, "A review on small scale wind turbines," *Renew. Sustain. Energy Rev.*, vol. 56, pp. 1351–1371, Apr. 2016.
- [2] J. Wang *et al.*, "Energy harvesting from flow-induced vibration: a lumped parameter model," *Energy Sources, Part A Recover. Util. Environ. Eff.*, vol. 40, no. 24, pp. 2903–2913, Dec. 2018.
- [3] J. Wang, L. Geng, L. Ding, H. Zhu, and D. Yurchenko, "The state-of-the-art review on energy harvesting from flow-induced vibrations," *Appl. Energy*, vol. 267, p. 114902, Jun. 2020.
- [4] J. Wang, Y. Zhang, M. Liu, and G. Hu, "Etching metasurfaces on bluff bodies for vortex-induced vibration energy harvesting," *Int. J. Mech. Sci.*, vol. 242, p. 108016, Mar. 2023.
- [5] H. L. Dai, A. Abdelkefi, and L. Wang, "Theoretical modeling and nonlinear analysis of piezoelectric energy harvesting from vortex-induced vibrations," *Int. J. Mech. Sci.*, vol. 25, no. 14, pp. 1861–1874, Jun. 2014.
- [6] M. Mohiuddin, K. M. Rahman, Z. Ahmed, and R. Ahmed, "Optimizing Power Density in Partially Coated Cantilever Beam Energy Harvesters: A Cost-Effective Design Strategy," *Energies 2024, Vol. 17, Page 5572*, vol. 17, no. 22, p. 5572, Nov. 2024.
- [7] M. Mohiuddin, Z. U. Ahmed, and R. Ahmed, "Influence of Beam Geometry on the Power Capacity of a Cantilever Beam Based Energy Harvester," Vol. 6 Dyn. Vib. Control, Feb. 2024.
- [8] M. Mohiuddin, Z. U. Ahmed, and R. Ahmed, "An

- Analysis of Concave and Convex Shaped Cantilever Beams On Vibration-Based Piezoelectric Energy Harvesting," Vol. 11 36th Conf. Mech. Vib. Sound, Nov. 2024.
- [9] V. Azadeh-Ranjbar, N. Elvin, and Y. Andreopoulos, "Vortex-induced vibration of finite-length circular cylinders with spanwise free-ends: Broadening the lock-in envelope," *Phys. Fluids*, vol. 30, no. 10, Oct. 2018.
- [10] Y. Gao, Z. Zhang, L. Zou, L. Liu, and B. Yang, "Effect of surface roughness and initial gap on the vortex-induced vibrations of a freely vibrating cylinder in the vicinity of a plane wall," *Mar. Struct.*, vol. 69, p. 102663, Jan. 2020.
- [11] S. Huang, "VIV suppression of a two-degree-of-freedom circular cylinder and drag reduction of a fixed circular cylinder by the use of helical grooves," *J. Fluids Struct.*, vol. 27, no. 7, pp. 1124–1133, Oct. 2011.
- [12] Z. Jin, G. Li, J. Wang, and Z. Zhang, "Design, modeling, and experiments of the vortex-induced vibration piezoelectric energy harvester with bionic attachments," *Complexity*, vol. 2019, 2019.
- [13] J. Wang, S. Sun, L. Tang, G. Hu, and J. Liang, "On the use of metasurface for Vortex-Induced vibration suppression or energy harvesting," *Energy Convers. Manag.*, vol. 235, p. 113991, May 2021.
- [14] J. Song, G. Hu, K. T. Tse, S. W. Li, and K. C. S. Kwok, "Performance of a circular cylinder piezoelectric wind energy harvester fitted with a splitter plate," *Appl. Phys. Lett.*, vol. 111, no. 22, Nov. 2017.
- [15] J. Wang, G. Zhao, M. Zhang, and Z. Zhang, "Efficient study of a coarse structure number on the bluff body during the harvesting of wind energy," *Energy Sources, Part A Recover. Util. Environ. Eff.*, vol. 40, no. 15, pp. 1788–1797, Aug. 2018.
- [16] G. Hu, K. T. Tse, K. C. S. Kwok, J. Song, and Y. Lyu, "Aerodynamic modification to a circular cylinder to enhance the piezoelectric wind energy harvesting," *Appl. Phys. Lett.*, vol. 109, no. 19, Nov. 2016
- [17] H. Zheng and J. Wang, "Galloping oscillation of a circular cylinder firmly combined with different shaped fairing devices," *J. Fluids Struct.*, vol. 77, pp. 182–195, Feb. 2018.
- [18] M. Mohiuddin, Z. U. Ahmed, A. Rahman, and M. R. Islam, "Performance Enhancement of Flow-Induced Energy Harvester through Integration of Semi-Circular Passive Turbulence Control," 2024.
- [19] G. Hu, K. T. Tse, M. Wei, R. Naseer, A. Abdelkefi, and K. C. S. Kwok, "Experimental investigation on the efficiency of circular cylinder-based wind energy harvester with different rod-shaped attachments," *Appl. Energy*, vol. 226, pp. 682–689, Sep. 2018.